

Supporting Information:

CO and CO₂ Adsorption Mechanism in Fe(pz)[Pt(CN)₄] Probed by Neutron Scattering and Density-Functional Theory Calculations

Ángel Fernández-Blanco,^{†,‡} Lucía Piñeiro-López,[¶] Mónica Jiménez-Ruiz,[†]
Stephane Rols,[†] José Antonio Real,[§] Jose Sanchez Costa,[¶] Roberta Poloni,^{*,||} and
J. Alberto Rodríguez-Velamazán^{*,†}

[†]*Institut Laue Langevin, 71 Avenue des Martyrs, CS 20156-38042, Grenoble, France*

[‡]*University of Grenoble-Alpes, SIMaP, F-38042, Grenoble, France*

[¶]*IMDEA Nanociencia, Faraday 9, Ciudad Universitaria de Cantoblanco, 28049, Madrid,
Spain*

[§]*Departamento de Química Inorgánica, Instituto de Ciencia Molecular (ICMol),
Universidad de Valencia, 46980, Paterna, Spain*

^{||}*University of Grenoble-Alpes, SIMaP, Grenoble-INP, CNRS, F-38042 Grenoble, France*

E-mail: roberta.poloni@grenoble-inp.fr; velamazan@ill.eu

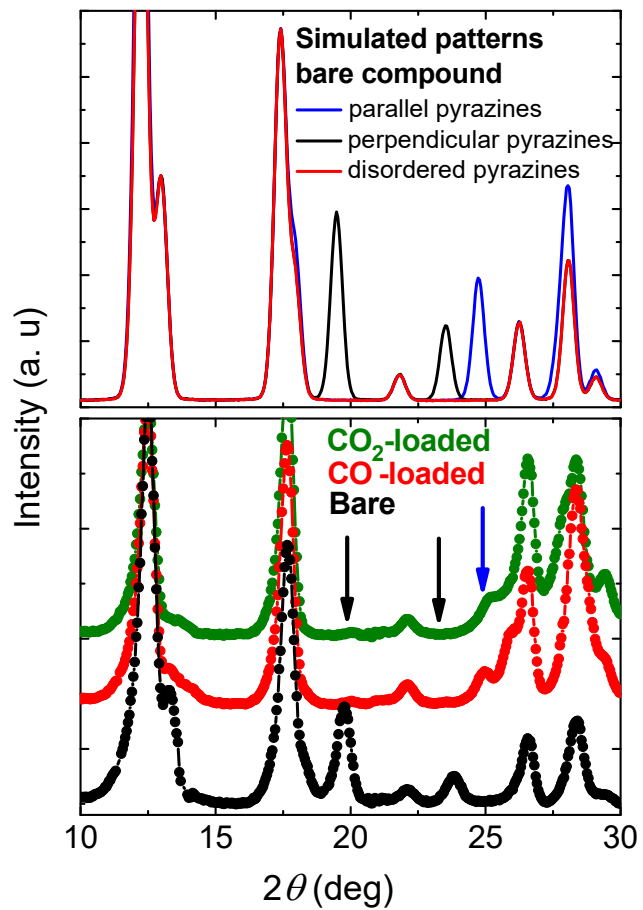


Figure S1: Top: Detail of the low Q part of the simulated neutron powder diffraction patterns (wavelength 1.54 Å) of $\text{Fe}(\text{d}_4\text{-pyrazine})[\text{Pt}(\text{CN})_4]$ in the low-spin state with the pyrazine rings in disordered (red lines), perpendicular (black lines) and parallel (blue lines) configurations. Bottom: Experimental neutron diffraction patterns of the CO (red), CO_2 -loaded (green) and bare (black) $\text{Fe}(\text{d}_4\text{-pyrazine})[\text{Pt}(\text{CN})_4]$. The arrows indicate the position of the reflections related to the different configurations of the pyrazine moieties: perpendicular (black lines) and parallel (blue lines)

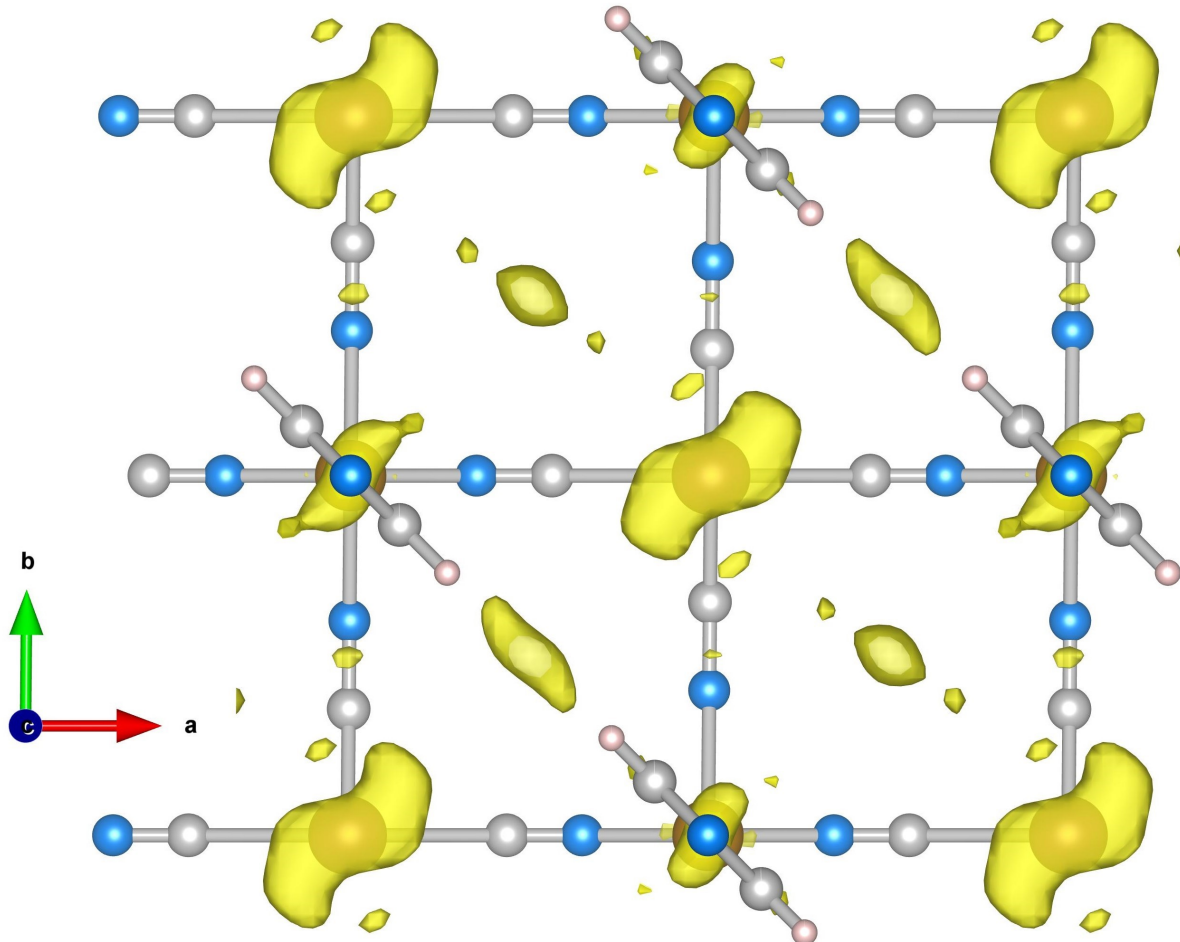


Figure S2: Residual scattering density in the ab plane when a model of the bare $\text{Fe}(\text{pyrazine})[\text{Pt}(\text{CN})_4]$ with parallel pyrazines is compared to the experimental neutron diffraction pattern of the CO-loaded compound. Two bonding sites for the CO are distinguished: (i) On top of the open-metal site (platinum site, site A) and (ii) in-between the pyrazine rings (pyrazine site, site B). The residual scattering density corresponding to site A is located at a distance of around 3.4 \AA from the open metal site along the z -axis, in the middle of the distance between two Pt atoms. This distance gives a suggestion of the weak interaction of the adsorbed molecules. Site B, in turn, is located between the pyrazine molecules, at a distance of around 3.6 \AA in the xy -plane from the center of the rings. The shape of the residual scattering density at the binding sites is indicative of the disorder of the guest molecules at the measurement temperature. The residual density on the pyrazine molecules is an indication of orientational disorder of the rings.

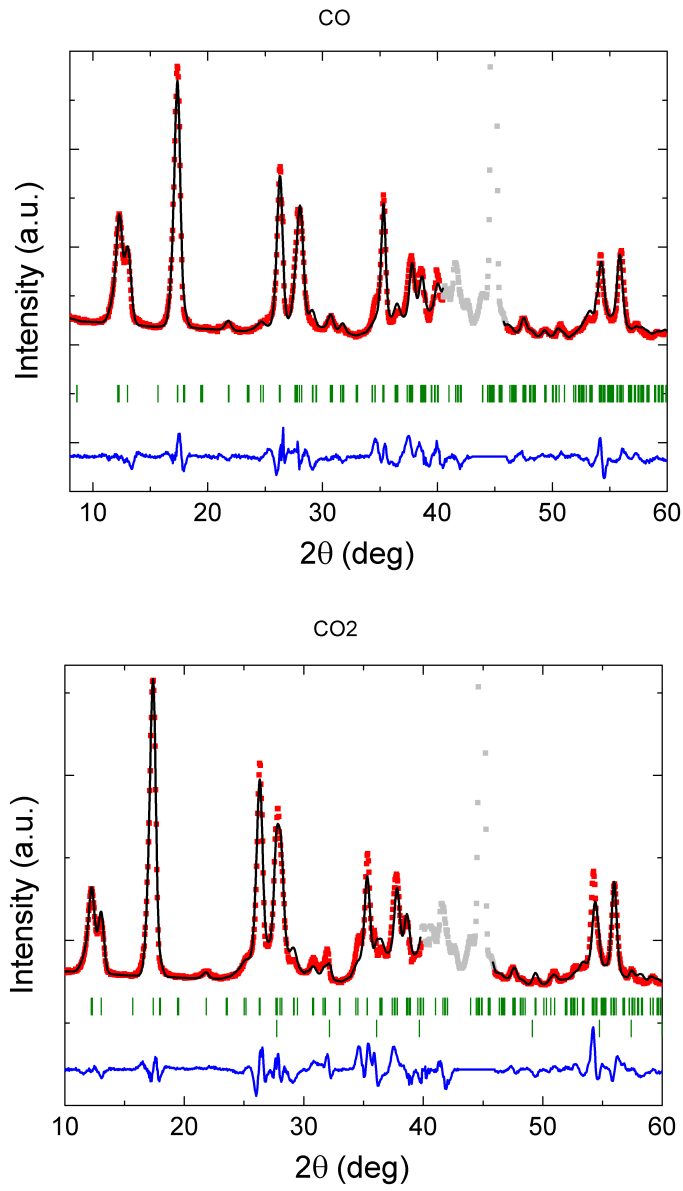


Figure S3: Details of the most relevant part of the powder neutron diffraction patterns (wavelength 1.54 Å) of Fe(pyrazine)[Pt(CN)4] loaded with CO (upper panel) and CO₂ lower panel. Experimental patterns (red), calculated patterns (black), difference patterns (blue lines), and position of the Bragg reflections (green marks). The parts in gray are regions with spurious scattering from the sample environment. A minor phase of solid CO₂ is also included in the case of the CO₂-loaded material (green marks in the lower line). The structural models were built in $P - 1$ space group, allowing distortion of the unit cell, but the atomic displacements were constrained to maintain a pseudo-tetragonal symmetry. The configuration of the pyrazine rings was fixed from the results obtained in the deuterated compound. For the CO-loaded material, full occupation of both A and B sites gave the best fits. For CO₂ the A site was considered fully occupied while the occupancy of guest molecules in the B site was allowed to vary. The refinement of the disorder among the possible orientations of the guest molecules did not give significant improvement of the fits, thus the disordered configurations were retained.

Table S1: Metric parameters obtained from the refinement of the powder neutron diffraction patterns of CO- and CO₂-loaded Fe(pyrazine)[Pt(CN)₄].

Compound	CO-loaded	CO ₂ -loaded
T(K)	100	100
Spin state	Low-spin	Low-spin
Space group	<i>P</i> - 1	<i>P</i> - 1
<i>a</i> (Å)	10.166(1)	10.164(1)
<i>b</i> (Å)	10.138(1)	10.136(1)
<i>c</i> (Å)	6.756(1)	6.753(1)
γ (°)	89.56(1)	89.68(2)
R_{Bragg}	13.95	17.33

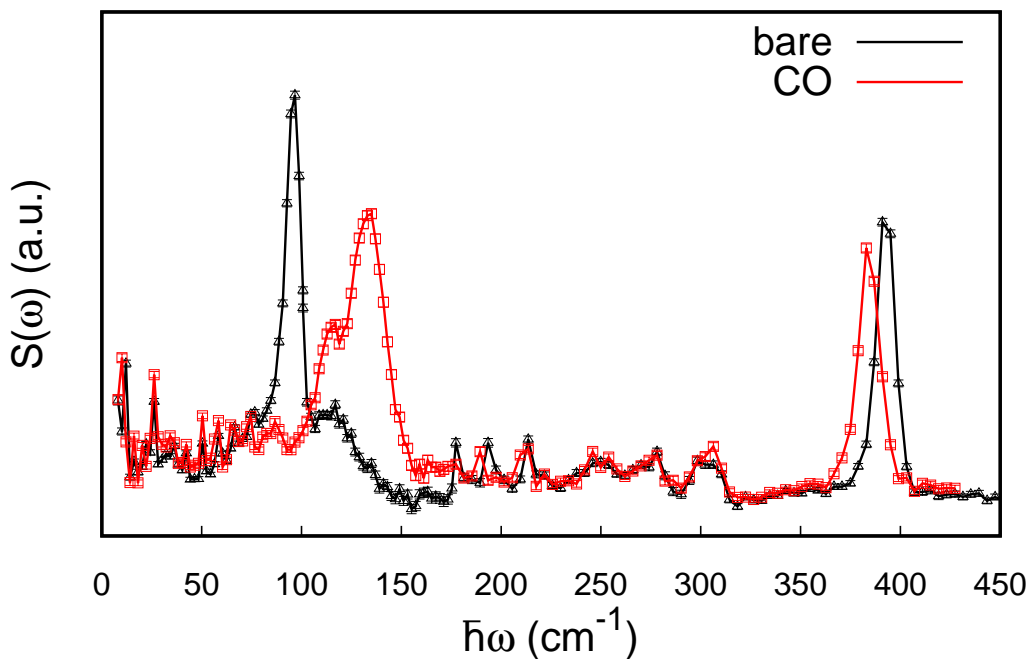


Figure S4: INS spectra (and errors) measured at IN1-LAGRANGE at 30 K for the empty Fe(pz)[Pt(CN)₄] (black) and after CO adsorption (red).

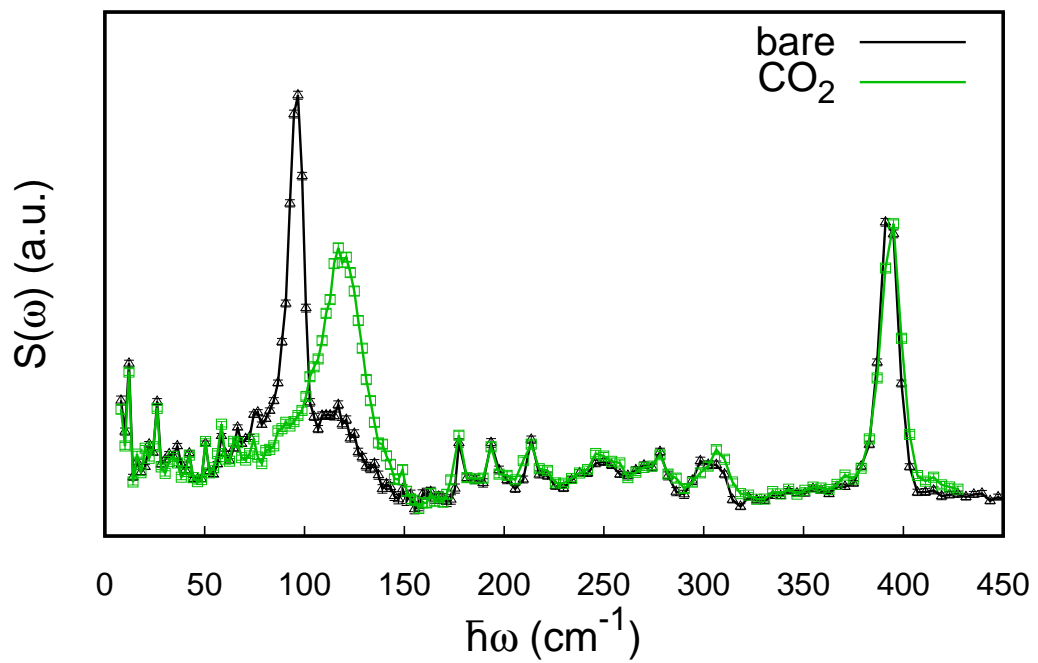


Figure S5: INS spectra (and errors) measured at IN1-LAGRANGE at 30 K for the empty $\text{Fe}(\text{pz})[\text{Pt}(\text{CN})_4]$ (black) and after CO_2 adsorption (green).

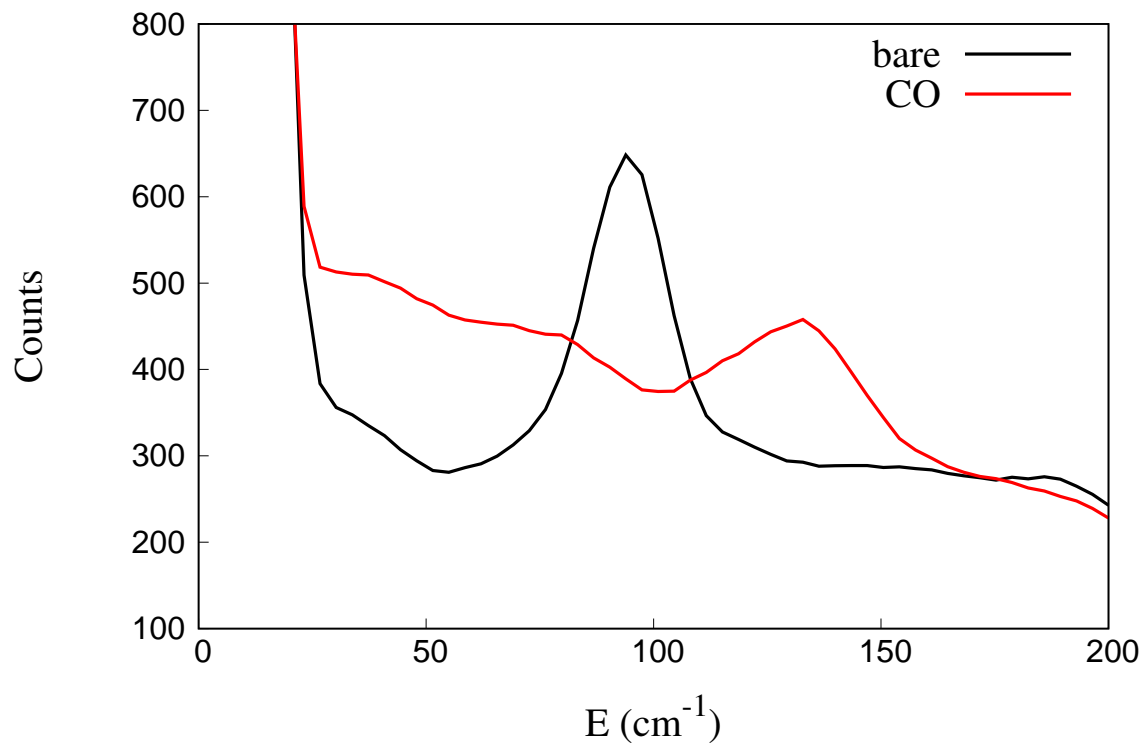


Figure S6: INS data collected at 10 K on PANTHER for the bare and loaded material with CO.

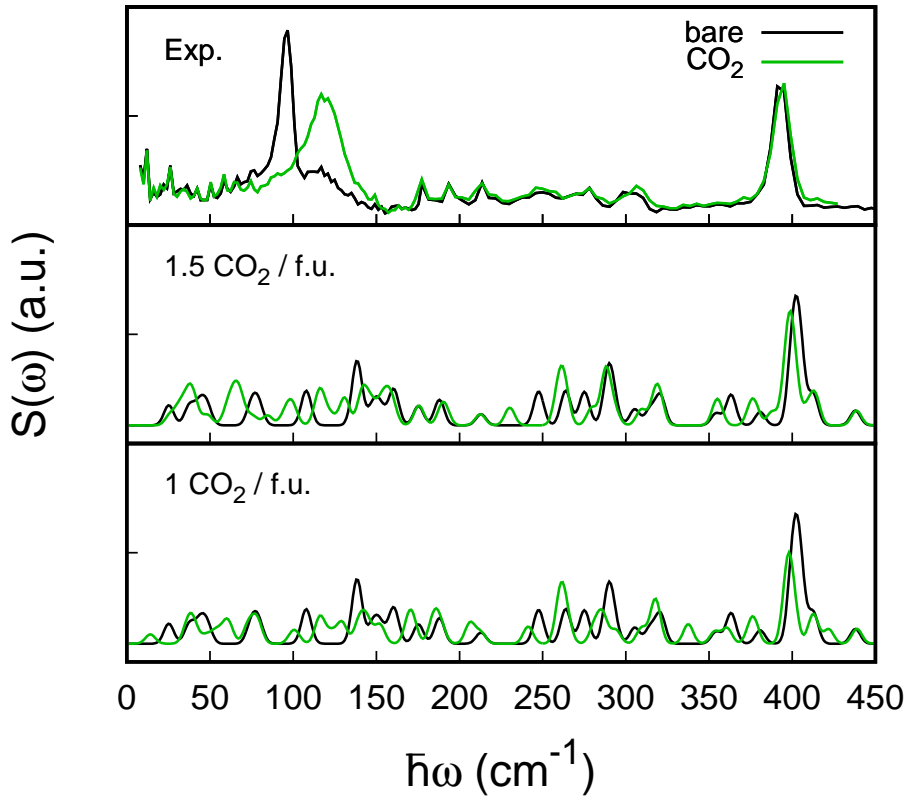


Figure S7: INS spectra measured at IN1 at 30 K for the empty Fe(pz)[Pt(CN)₄] (black) and after CO₂ adsorption (green) in the upper panel. Total S(ω) computed for 1.5 and 1 CO₂ per f.u., respectively, in the lower panels. The displacement of the most intense modes at 107.9, 17.8, 138.5 and 139.2 cm^{-1} are approximately similar for both cases. The peak around 400 cm^{-1} does not undergo any displacement in any case.

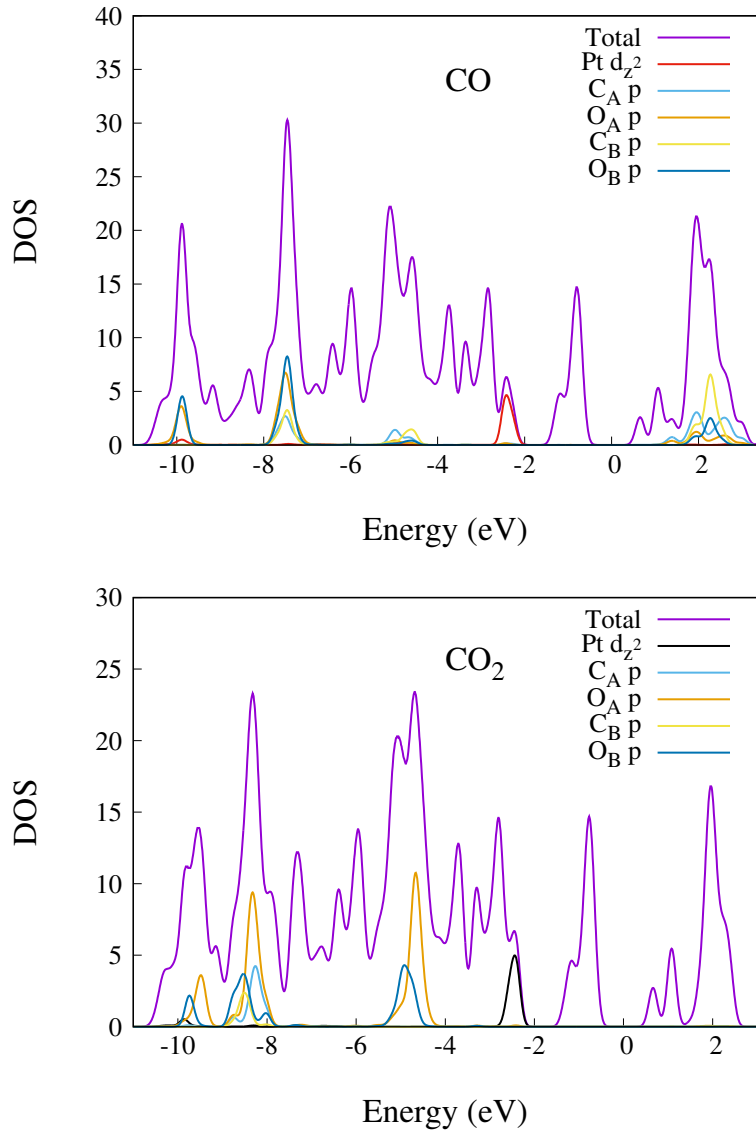


Figure S8: Total and projected (onto the Pt d_{z^2} and the p atomic orbitals of CO and CO_2) DOS computed for the MOF+CO (2 CO/f.u.) (upper panel) and MOF+ CO_2 (1.5 CO_2 /f.u.) (lower panel). The labels A and B represent the bonding site A (platinum site) or B (pyrazine site), respectively. The Fermi level is set to 0 eV. For CO (upper panel) a bonding interaction between σ -HOMO orbital of the CO and the Pt- d_{z^2} orbital is found at -5.1 and -4.9 eV. The corresponding antibonding interaction appears at -2.3 eV.

Table S2: Comparison of the binding energies (eV) and C_A -Pt bond distances (\AA) computed using different functionals. C_A stands for the carbon atom of the molecule on site A. ^a Optimized geometry from PBE+D2. ^b Full relaxation.

	SO ₂		CO		CO ₂	
	E_{bind}	d(S-Pt)	E_{bind}	d(C _A -Pt)	E_{bind}	d(C _A -Pt)
PBE	0.239	2.90	0.029	3.39	0.002	3.44
PBE+D2	0.769	2.93	0.278	3.37	0.435	3.39
PBE+D2+U ^a	0.617	2.93	0.283	3.37	0.453	3.39
PBE+D2+U ^b	0.683	3.47	0.276	3.43	0.440	3.44
PBE+D2[U] ^a	0.730	2.93	0.284	3.37	0.445	3.39
PBE+D2[U] ^b	0.719	3.47	0.289	3.43	0.452	3.44